The Journal of Immunology

Targeting the Neonatal Fc Receptor for Antigen Delivery Using Engineered Fc Fragments

Wentao Mi, Sylvia Wanjie, Su-Tang Lo, Zhuo Gan, Beatrix Pickl-Herk, Raimund J. Ober and E. Sally Ward

J Immunol 2008; 181:7550-7561; ;
doi: 10.4049/jimmunol.181.11.7550
http://www.jimmunol.org/content/181/11/7550

The Journal of Immunology is published twice each month by
The American Association of Immunologists, Inc.,
9650 Rockville Pike, Bethesda, MD 20814-3994.

Print ISSN: 0022-1767 Online ISSN: 1550-6606.

Targeting the Neonatal Fc Receptor for Antigen Delivery Using Engineered Fc Fragments[1]

Wentao Mi,* Sylvia Wanjie,* Su-Tang Lo,* Zhuo Gan,* Beatrix Pickl-Herk,* Raimund J. Ober,*† and E. Sally Ward[2]*

The development of approaches for Ag delivery to the appropriate subcellular compartments of APCs and the optimization of Ag persistence are both of central relevance for the induction of protective immunity or tolerance. The expression of the neonatal Fc receptor, FcRn, in APCs and its localization to the endosomal system suggest that it might serve as a target for Ag delivery using engineered Fc fragment-epitope fusions. The impact of FcRn binding characteristics of an Fc fragment on in vivo persistence allows this property to also be modulated. We have therefore generated recombinant Fc (mouse IgG1-derived) fusions containing the N-terminal epitope of myelin basic protein that is associated with experimental autoimmune encephalomyelitis in H-2^u mice. The Fc fragments have distinct binding properties for FcRn that result in differences in intracellular trafficking and in vivo half-lives, allowing the impact of these characteristics on CD4$^+$ T cell responses to be evaluated. To dissect the relative roles of FcRn and the "classical" FcγRs in Ag delivery, analogous aglycosylated Fc-MBP fusions have been generated. We show that engineered Fc fragments with increased affinities for FcRn at pH 6.0–7.4 are more effective in delivering Ag to FcRn-expressing APCs in vitro relative to their lower affinity counterparts. However, higher affinity of the FcRn-Fc interaction at near neutral pH results in decreased in vivo persistence. The trade-off between improved FcRn targeting efficiency and lower half-life becomes apparent during analyses of T cell proliferative responses in mice, particularly when Fc-MBP fusions with both FcRn and FcγR binding activity are used. *The Journal of Immunology,* **2008, 181: 7550–7561.**

The delivery of Ag to elicit protective immunity or tolerance represents an area of considerable interest for both vaccine development and the treatment of autoimmunity (1–4). For CD4$^+$ T cell responses, a primary goal is to achieve efficient delivery of Ag to the site of peptide loading onto MHC class II molecules, namely the endolysosomal system of APCs (5). However, there is an incomplete understanding as to how the intracellular trafficking pathways of an Ag impact presentation and how this can be modulated. How Ag persistence, which relates to intracellular trafficking, affects both qualitative and quantitative aspects of CD4$^+$ T cell responses is also of fundamental importance for understanding the factors that regulate T cell-mediated immunity. Toward addressing these issues, here we use an approach in which we exploit properties of the MHC class I-related neonatal Fc receptor (FcRn)[3] to modulate the uptake/intracellular trafficking and in vivo half-life of Ag as intrinsic properties of the delivery vehicle.

Fc receptors that bind to the Fc region of IgG encompass the classical Fc receptors (FcγRs) and FcRn that can be distinguished in several important ways. The FcγRs are signaling receptors that can transmit activating or inhibitory signals depending upon whether they associate with the ITAM containing Fcγ chain or have cytosolic ITIM motifs (6, 7). Conversely, the MHC class I-related receptor FcRn has no known signaling role and serves as an IgG transporter to maintain Ab levels in vivo (8–14). The expression patterns of FcγRs and FcRn also differ, since FcγRs are primarily expressed by cells of hematopoietic origin (15–17), whereas FcRn is ubiquitously present in cells of diverse origin such as endothelial and epithelial cells (11, 13, 18–20). However, both FcRn and FcγRs are expressed in professional APCs such as dendritic cells (DCs) and macrophages (17, 21–23). Although the role of FcγRs in Ag uptake and presentation is well documented (16, 24–26), there is very limited knowledge concerning a possible function for FcRn.

FcRn transports IgGs within and across cells, and the interaction properties of an IgG with FcRn are key determinants of its in vivo persistence (27–30). The binding of naturally occurring IgGs to FcRn is pH dependent, with relatively strong binding at pH 6.0 that becomes progressively weaker as pH 7.3–7.4 is approached (31–34). The model for FcRn-mediated transport of IgG is as follows: IgGs are taken into cells by fluid phase uptake and enter endosomes where the acidic pH is permissive for binding. IgG molecules that bind to FcRn are recycled or transcytosed, whereas those that do not interact enter lysosomes (35). In contrast with FcRn, in general FcγRs transport bound ligands in the form of immune complexes into degradative compartments that can be involved in Ag presentation within cells (16, 24, 25), although FcγRIIB-mediated Ag recycling has also been observed in DCs (36). The interaction sites for FcRn and FcγRs on IgGs are distinct (37–40) and, unlike FcγR-IgG interactions, FcRn binding is not affected by removal of N-linked glycosylation on the CH2 domain (27, 38,

*Department of Immunology, University of Texas Southwestern Medical Center, Dallas, TX 75390; and †Department of Electrical Engineering, University of Texas at Dallas, Richardson, TX 75080

Received for publication July 3, 2008. Accepted for publication September 25, 2008.

The costs of publication of this article were defrayed in part by the payment of page charges. This article must therefore be hereby marked *advertisement* in accordance with 18 U.S.C. Section 1734 solely to indicate this fact.

[1] This work was supported in part by grants from the National Multiple Sclerosis Society (RG 2411) and the National Institutes of Health (AI/NS ROI 42949).

[2] Address correspondence and reprint requests to Dr. E. Sally Ward, Department of Immunology, University of Texas Southwestern Medical Center, 6000 Harry Hines Boulevard, Dallas, TX 75390-9093. E-mail address: Sally.Ward@UTsouthwestern.edu

[3] Abbreviations used in this paper: FcRn, neonatal Fc receptor; Abdegs, Abs that enhance IgG degradation; β_2m, β_2-microglobulin; CHO, Chinese hamster ovary; DC, dendritic cell; EAE, experimental autoimmune encephalomyelitis; MBP, myelin basic protein; mDC, myeloid dendritic cell; tg, transgenic; WT, wild type.

41). This allows the relative contributions of FcγRs and FcRn to functional effects to be evaluated.

The present study is directed toward evaluating a possible role for FcRn in Ag delivery and presentation. As a consequence of the function of FcRn in regulating IgG/Fc persistence, this also enables an analysis of the impact of Ag persistence on cognate $CD4^+$ T cell responses. Central to our studies are a class of engineered IgGs that, relative to their wild-type counterparts, bind to FcRn with increased affinities in the pH range 6.0–7.4 (29, 30, 42). Compared with wild-type IgGs, we have shown previously that these Abs accumulate to high levels in FcRn-expressing cells since they can be taken up by receptor-mediated endocytosis and are inefficiently released at the cell surface during exocytic events (30, 42, 43). Such IgGs can lower endogenous IgG levels in vivo by competing for FcRn binding. However, IgGs (or Abdegs, for Abs that enhance IgG degradation) of this class also have short in vivo half-lives (29, 30). Herein we show that in contrast to wild-type IgGs that are recycled (35), these mutated variants enter lysosomes following uptake into cells. The accumulation of Abdegs in the endolysosomal pathway, together with the expression of FcRn in APCs (23), has prompted us to compare the $CD4^+$ T cell stimulatory properties of engineered Fc fragments that differ in both intracellular trafficking behavior and in vivo persistence.

For use in our studies, we have generated Fc fusion proteins with distinct FcRn binding properties that are linked to the N-terminal epitope of myelin basic protein (MBP), MBP1–9. This peptide represents the immunodominant epitope of MBP in $H\text{-}2^u$ mice and is associated with autoreactive $CD4^+$ T cell responses that can culminate in experimental autoimmune encephalomyelitis (EAE) (44). Covalent Fc-epitope fusions have been used in preference to noncovalent Ab-Ag complexes to avoid possible complications of Ag/epitope dissociation. To assess the contribution of the classical FcγRs to the outcome, the activities of engineered Fc fusions that do, and do not, bind to this class of receptors have also been compared. Our studies demonstrate that targeting FcRn with Abdegs can enhance Ag delivery and presentation using in vitro assays for which Ag persistence does not play a role. This enhancement can also be revealed during analyses of T cell proliferative responses in vivo when binding to FcγRs is excluded. However, when FcγR-competent fusions are used, the counterbalancing impact of reduced in vivo half-life of Abdegs becomes apparent and longer lived Fc-MBP fusions are more effective.

Materials and Methods

Mice

B10.PL ($H\text{-}2^u$) mice were purchased from The Jackson Laboratory. Mice that transgenically express the 1934.4 TCR (1934.4 tg mice; Ref. 45) or clone 19 TCR (T/R+ tg mice; Ref. 46) were kindly provided by Dr. Hugh McDevitt (Stanford University, Palo Alto, CA) and Dr. Juan Lafaille (New York University School of Medicine, New York, NY), respectively. Both the 1934.4 and clone 19 TCRs are specific for MBP1–9 complexed with $I\text{-}A^u$ (45, 46) and have similar affinities and in vitro responsiveness (our unpublished data). Transgenic (tg) mice were maintained by backcrossing onto B10.PL mice. All mice were housed and handled in pathogen-free animal facilities in compliance with institutional policies and guidelines and Institutional Animal Care and Use Committee-approved protocols. Male or female mice of 6–9 wk old were used in experiments.

Cell lines

The MBP1–9:$I\text{-}A^u$-specific T hybridoma, 46, was generated from mice that transgenically express the β-chain of the 172.10 TCR (47) following immunization with 200 μg MBP1–9[4Y] (MBP1–9 with lysine at position 4 substituted by tyrosine) and methods described previously (48). The $I\text{-}A^u$-expressing B lymphoblastoid line PL-8 and 1934.4 hybridoma (49) were generously provided by Dr. David Wraith (University of Bristol, Bristol, U.K.), and the 172.10 hybridoma (47) was provided by Dr. Joan Goverman (University of Washington, Seattle). Stable transfectants of PL-8 cells expressing mouse FcRn tagged with GFP (PL-8:FcRn) were generated by transfection of PL-8 cells with a mouse FcRn-GFP construct (42) followed by selection with G418 (600 μg/ml, Invitrogen).

Production of mouse Fc-MBP fusions and fluorescence labeling

A previously described construct encoding the wild-type (WT) mouse hinge-Fc region (mouse IgG1 derived) tagged with a C-terminal polyhistidine tag (50) was modified to generate the following derivatives: the WT Fc-hinge (Fc-WT) gene was mutated using splicing by overlap extension (51) to insert the following mutations to generate Fc-mut: Thr^{252} to Tyr, Thr^{256} to Glu, His^{433} to Lys, and Asn^{434} to Phe. Codons encoding Gly-Ser-Gly-Gly and the MBP1–9[4Y] peptide were inserted as overlapping oligonucleotides into a unique *Bst*EII site at the 3′ end of the Fc-WT or Fc-mut genes (5′ to the polyhistidine tag) using standard methods of molecular biology. The Fc-WT gene was subsequently mutated by splicing by overlap extension to insert the H435A mutation, which has been shown previously to ablate binding of human IgG1 to FcRn (52). The resulting three constructs containing Fc-WT, Fc-mut, and Fc-H435A linked to MBP1–9[4Y] were then further modified by replacing the prokaryotic pelB leader sequence (50) by the native mouse IgG1 leader peptide using overlapping oligonucleotides and the PCR. *Bam*HI sites were appended at the 5′ and 3′ ends of the Fc-MBP fusion genes, and they were ligated into *Bam*HI-restricted pEF6/V5-His vector (Invitrogen). These constructs were further mutated using splicing by overlap extension to insert the N297A mutation. Fc-WT-MBP(3A6A) was made by inserting oligonucleotides encoding Gly-Ser-Gly-Gly and the MBP1–9[4Y] peptide with Gln^3 to Ala, Pro^6 to Ala as overlapping oligonucleotides into a unique *Bst*EII site at the 3′ end of the Fc-WT gene. All constructs were sequenced before use in transfections of Chinese hamster ovary (CHO) cells. Stable transfectants were selected in CD CHO cell medium (Invitrogen) containing 8 μg/ml blasticidin (Invitrogen).

The Fc-MBP fusions were purified from culture supernatants using Ni^{2+}-NTA-agarose columns and previously described methods (50). Purified Fc-MBP fusions were labeled with Alexa 647 using Alexa Fluor 647 succimidyl ester (Molecular Probes) and methods recommended by the manufacturer.

Surface plasmon resonance analyses

Equilibrium dissociation constants of the Fc-MBP fusions for mouse FcRn were determined using surface plasmon resonance and a BIAcore 2000 as described previously (53, 54). Fc-MBP fusions were immobilized by amine coupling chemistry to a density of ~500 resonance units. Recombinant mouse FcRn was purified from baculovirus-infected High Five cells (53) and was used as analyte in PBS plus 0.01% Tween (pH 6.0 or 7.4). IgG or Fc has two possible interaction sites, and equilibrium binding data were fitted as described elsewhere (54). The dissociation constants for the higher affinity interaction sites are presented.

Recombinant peptide-MHC complexes

Soluble, recombinant MBP peptide:$I\text{-}A^u$ (MBP1–9[4Y]:$I\text{-}A^u$) complexes were generated and purified using baculovirus-infected High Five cells, and multimeric complexes ("tetramers") were generated using PE-labeled ExtrAvidin (Sigma-Aldrich) (55).

Flow cytometry reagents and analyses

Single-cell suspensions were obtained from homogenized spleens or regional lymph nodes (inguinal and intestinal lymph nodes) as described previously (56). The following fluorescently labeled Abs were purchased from BD Biosciences and used for flow cytometry: FITC-labeled anti-CD11b (M1/70), PE-labeled anti-CD4 (GK1.5), Vβ8 TCR (F23.1), B220 (RA3-6B2), CD11c (HL3), PerCP-labeled anti-B220 (RA3-6B2), CD4 (RM4-5), Gr-1 (RB6-8C5), and allophycocyanin-labeled anti-CD4 (RM4-5), CD62L (MEL-14), and CD19 (1D3). PE-labeled anti-F4/80 (BM8) was purchased from Invitrogen. Anti-Vβ8 (F23.1) Ab was purified from culture supernatants of the F23.1 hybridoma using protein G-Sepharose and fluorescently labeled with Alexa Fluor 647 succimidyl ester according to the manufacturer's instructions. Anti-$I\text{-}A^u$ Ab was purified from the 10.2.16 hybridoma and labeled with fluorescein-isothiocyanate using standard methods. Cells were treated with fluorescently labeled tetramers or Abs (56). Flow cytometry analyses were performed using a FACSCalibur (BD Biosciences) and data analyzed using FlowJo (Tree Star).

Uptake and accumulation of Fc-MBP fusions in cells

PL-8 cells, PL-8:FcRn cells, or splenocytes were pulsed with 2–5 μg/ml Alexa 647-labeled Fc-MBP fusions in prewarmed phenol red free, IgG-depleted cDMEM (DMEM (Lonza) supplemented with 10% IgG-depleted

FCS, 100 μM nonessential amino acids, 1 mM sodium pyruvate, 55 μM 2-ME, 10 mM HEPES (pH 7.2–7.5)) at 37°C for 20–30 min, washed, or chased following the washes in prewarmed medium at 37°C for 30 min (30, 42). Following these treatments with Alexa 647-labeled Fc-MBP fusions, splenocytes were incubated on ice with fluorescently labeled Abs to identify cell populations as follows: macrophages ($CD11b^{int+}F4/80^{+}$), myeloid DCs (mDCs, $CD11b^{+}CD11c^{+}B220^{-}$), and B cells ($B220^{+}I\text{-}A^{u+}$). Labeled cells were analyzed by flow cytometry as above. The role of FcγRs in uptake of Fc-MBP fusions was determined by incubating PL-8 cells, PL-8:FcRn cells, or splenocytes with 5 μg/ml anti-FcγRIIB/III Ab (2.4G2) or isotype-matched rat IgG2b at 4°C for 15 min before addition of Fc-MBP fusions.

RT-PCR analyses

Single-cell suspensions derived from splenocytes were stained with PE-labeled anti-B220 (RA3-6B2) and allophycocyanin-labeled anti-CD19 (1D3) and B cells were sorted by FACS using a MoFlo (Beckman Coulter). Total RNA was isolated from cells using RNA-Bee (Tel-Test) and standard methods. cDNA synthesis was conducted using two forward oligonucleotide primers complementary to the 3′ ends of the FcRn (57) and β_2-microglobulin (β_2m) genes (FcRn forward, 5′-AGA AGT GGC TGG AAA GGC ATT TGC ACC-3′; β_2m forward, 5′-CAT GTC TCG ATC CCA GTA GAC GGT CTT-3′). cDNA was used in PCRs with corresponding reverse primers (FcRn reverse, anneals to bases 679–705, 5′-TAC CCA CCG GAG CTC AAG TTT CGA TTC-3′; β_2m reverse, anneals to bases 1–27, 5′-ATG GCT CGC TCG GTG ACC CTG GTC TTT-3′). PCRs were run for 30 cycles under standard conditions and the 415-bp PCR product corresponding to the 3′ end of the FcRn α-chain gene was gel-purified and sequenced.

Fluorescence microscopy

PL-8:FcRn cells were seeded in 24-well plates containing coverslips (Fisherbrand 1.5; Fisher Scientific) overnight. PL-8:FcRn cells were incubated with 500 μg/ml Alexa 555-labeled dextran (10,000 molecular mass, Invitrogen) in phenol red-free, IgG-depleted cDMEM for 2 h at 37°C. Cells were then washed and chased in medium for 1 h. Fc-MBP fusions (5 μg/ml in medium) were subsequently added and cells were incubated at 37°C for different times. Cells were washed, fixed with 3.4% paraformaldehyde, and mounted (35). Cells were imaged using two microscopy setups for Fig. 4, *A* and *B*, respectively: a Zeiss Axiovert 200M inverted fluorescence microscope with a Zeiss 1.4 NA/100× Plan-Apochromat objective and a Zeiss 1.6× Optovar (42); a Zeiss Axiovert S100TV inverted fluorescence microscope with a Zeiss 1.4 NA/100× Plan-Apochromat objective and a Zeiss 1.6× Optovar (35, 43). All data were processed and displayed using the custom-written microscopy image analysis tool (MIATool) software package (www4.utsouthwestern.edu/wardlab) in MATLAB (Mathworks). The intensities of acquired data were linearly adjusted. Images were overlaid and annotated. In overlay images, the intensities of the individual color channels were adjusted to similar levels.

ELISA and T cell proliferation assay

Different concentrations of Fc-MBP fusions were added to 96-well plates containing PL-8 or PL-8:FcRn cells (5×10^4 cells/well) and MBP1–9:I-A^u-specific T hybridoma cells (5×10^4 cells/well) or to 96-well plates containing splenocytes (3×10^5 cells/well) derived from 1934.4 tg mice (45) (as in Refs. 48, 56). IL-2 levels in culture supernatants and proliferative responses ([^{3}H]thymidine incorporation) were assessed (48, 56). Cultures were also set up in the presence of 5 μg/ml anti-FcγRIIB/III Ab (2.4G2) or isotype-matched control Ab (rat IgG2b) to assess FcγR-mediated effects.

In vivo proliferative responses of T cells

Splenocytes from 1934.4 tg mice were isolated and labeled with CFSE using previously described methods (56). The activation status of the $CD4^+$ T cells was assessed using anti-CD62L Ab and flow cytometry and the percentage of $CD62L^{lo}$ cells was <11% in all experiments. CD4 T cells (2×10^6, as mixtures in splenocytes) were transferred into B10.PL mice, and subsequently 100 ng of each Fc-MBP fusion was injected i.v. Three days later, splenocytes and regional lymph nodes were harvested and analyzed by flow cytometry using fluorescently labeled anti-CD4 Ab, anti-Vβ8 (F23.1) Ab, and PE-labeled MBP1–9[4Y]:I-A^u tetramers.

To examine the longevity of functional Ag:I-A^u complexes derived from Fc-MBP fusions in vivo, recipient B10.PL mice were injected i.v. with each Fc-MBP fusion (1 μg/mouse), and the mice were adoptively transferred with 2×10^6 $CD4^+$ T cells derived from 1934.4 tg mice, or combined from 1934.4 tg and T/R^+ tg mice, i.v. at 1 h, 3 days, and 7 days following Fc-MBP fusion treatment. Injections of Fc-MBP fusions were staggered over a 7-day period, so that all recipient mice were transferred with the same population of Ag-specific T cells. Three days following transfer, splenocytes and lymph nodes were harvested and analyzed by flow cytometry as above.

Table I. *Binding properties of wild-type Fc and wild-type/mutated Fc-MBP fusions*

Fc or Fc-MBP Fusion	Binding to FcRn (K_D, nM) pH 6.0	Binding to FcRn (K_D, nM) pH 7.4	Binding to FcγR (II, III)
Fc-WT[a]	188.2	N.B.[b]	+
Fc-WT-MBP	212.1	N.B.	+
AglyFc-WT-MBP	169.7	N.B.	−
Fc-mut-MBP	1.4	16.5	+
AglyFc-mut-MBP	1.1	19.8	−
Fc-H435A-MBP	N.B.	N.B.	+
AglyFc-H435A-MBP	N.B.	N.B.	−

[a] Fc-WT with no MBP epitope attached. Agly indicates aglycosylated.
[b] N.B., no detectable binding or affinity too low to determine.

Statistical analyses

Tests for statistical significance were conducted using the statistical toolbox of MATLAB (Mathworks) and the function "multcompare".

Results

Generation of Fc-MBP fusions with distinct FcR binding properties

Several different Fc-fusion proteins that vary in the Fc region (mouse IgG1-derived) sequence were expressed for use in these studies (Table I). The wild-type Fc (Fc-WT) was mutated to generate the TT-HN mutant (Fc-mut; Thr^{252} to Tyr, Thr^{256} to Glu, His^{433} to Lys, and Asn^{434} to Phe; analogous to a previously described human IgG1 mutant, or Abdeg; see Ref. 42) and H435A mutant (His^{435} to Ala). These mutants have different binding properties for mouse FcRn: Fc-mut has markedly increased affinity relative to Fc-WT at both pH 6.0 and 7.4, and H435A shows undetectable binding (Table I). Fc fragments were linked through their C termini via a Gly-Ser-Gly-Gly sequence to the MBP1–9[4Y] peptide to generate Fc-WT-MBP, Fc-mut-MBP, and Fc-H435A-MBP. The peptide variant MBP1–9[4Y] was used in preference to wild-type MBP1–9, since the position 4 substitution of lysine by tyrosine results in higher affinity binding to I-A^u (58, 59). Glycine was also appended to the N terminus of the MBP peptide to mimick the N-terminal acetyl group that is necessary for T cell recognition (55, 60).

The Fc-MBP fusions were expressed in both glycosylated and aglycosylated forms in transfected CHO cells. Aglycosylation was achieved by mutation of Asn^{297} to Ala (N297A), which ablates binding to the classical FcγRs (61, 62) without affecting FcRn interactions (27, 38, 41). Mouse Fc (or IgG1) binds to the low-affinity FcγRIIB and FcγRIII, but not to the high-affinity FcγRI nor to the recently described FcγRIV (63). In other systems, monomeric IgG-epitope fusions have been shown to have effects through binding to low-affinity FcγRs (64, 65). Additionally, we cannot exclude the possibility that our recombinant proteins contain low levels of aggregates, which are more effective than monomers in mediating signaling through low-affinity FcγRs. In the current study we have therefore compared the effects of glycosylated and aglycosylated Fc-MBP fusions.

FcRn-mediated uptake enhances in vitro T cell responses to Fc-MBP fusions

To analyze the impact of FcRn expression on T cell stimulation in vitro, we have used an I-A^u-expressing B lymphoblastoid cell line,

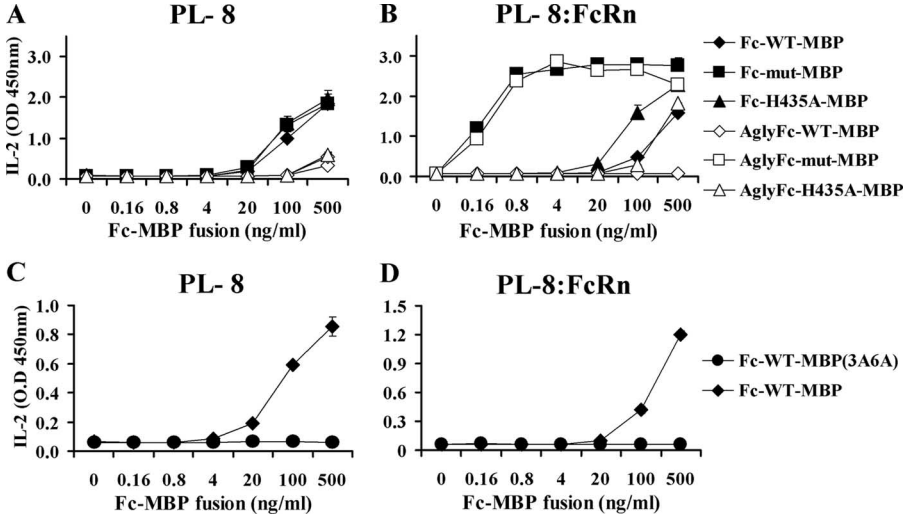

FIGURE 1. Responses of MBP1–9:I-A^u-specific T cell hybridoma 46 to Fc-MBP fusions. The data show IL-2 production following 24 h of incubation with Fc-MBP fusions in the presence of PL-8 (*A* and *C*) or PL-8:FcRn (*B* and *D*) cells as APCs. Error bars indicate SDs of triplicate samples. The data shown are representative of at least three independent experiments, except for *C*, which was conducted twice.

PL-8 (66), and FcRn-transfected PL-8 cells (PL-8:FcRn) as APCs. PL-8 cells were used since, by analogy with other in vitro B cell lines (8, 23), they do not express FcRn (our unpublished observations). Comparison of Ag presentation by PL-8 and PL-8:FcRn cells therefore allows the impact of FcRn expression to be assessed. In vitro stimulation of the MBP1–9:I-A^u-specific hybridoma, 46, with different Fc-MBP fusions results in distinct patterns of stimulation by the two types of APCs (Fig. 1, *A* and *B*). The TCR of hybridoma 46 is the same as that of the 172.10 hybridoma (47), with the exception of an Ala^{98} to Glu change in CDR3α (our unpublished data). In PL-8 cells, the stimulatory capacities of glycosylated Fc-WT-MBP, Fc-mut-MBP, and Fc-H435A-MBP are similar (Fig. 1*A*). However, this changes when the cells express FcRn, with the stimulatory activity decreasing in the order Fc-mut-MBP > Fc-H435A-MBP > Fc-WT-MBP (Fig. 1*B*). Similar results were observed for the 1934.4 (49) and 172.10 (47) hybridomas that are both specific for MBP1–9:I-A^u complexes (data not shown). Importantly, mutation of the T cell contact residues Gln^3 and Pro^6 in the MBP epitope (67) to alanine (MBP(3A6A)) results in loss of T cell stimulation, demonstrating the specificity of the T cell response (Fig. 1, *C* and *D*). Increasing the affinity of an Fc-MBP fusion for FcRn in the pH range 6.0–7.4 therefore enhances its ability to stimulate Ag-specific T cells when the APC expresses this Fc receptor. In contrast, the properties of Fc-WT most likely result in FcRn-mediated recycling (35, 43) of Fc-WT-MBP out of PL-8:FcRn cells. The stimulatory activities of glycosylated or aglycosylated Fc-H435A-MBP fall between those of Fc-mut-MBP and Fc-WT-MBP since these fusions do not accumulate via FcRn-mediated uptake and are not recycled out by FcRn-mediated processes.

In general, the glycosylated proteins were more stimulatory relative to the aglycosylated proteins when either PL-8 or PL-8:FcRn cells were used as APCs (Fig. 1, *A* and *B*). Since glycosylated, but not aglycosylated, proteins bind to FcγRs (61, 62), this suggested that FcγR interactions might be responsible for the increased activity. Mouse IgG1 can bind to FcγRIIB and FcγRIII but not to the high-affinity FcγRI, nor to FcγRIV (63). We therefore preincubated APCs with the anti-FcγR Ab 2.4G2, which binds to FcγRIIB, FcγRIII, and FcγRIV (15). Pretreatment with 2.4G2 reduced the levels of stimulation by the glycosylated proteins to those observed for their aglycosylated counterparts (Fig. 2), indicating that the differences are due to FcγR binding. Using RT-PCR, we observed that PL-8 cells express both FcγRIIB and FcγRIII (data not shown), indicating that one or both of these receptors are responsible for the enhanced activity of glycosylated Fc-MBP fusions.

We hypothesized that the increased stimulatory activity of Fc-mut-MBP relative to Fc-WT-MBP is due, at least in part, to increased accumulation in APCs. The uptake and retention of fusion proteins containing Fc-mut or Fc-WT by PL-8 and PL-8:FcRn cells in medium at 37°C were therefore compared (Fig. 3). Alexa 647-labeled Fc-MBP fusions were added at concentrations of 2

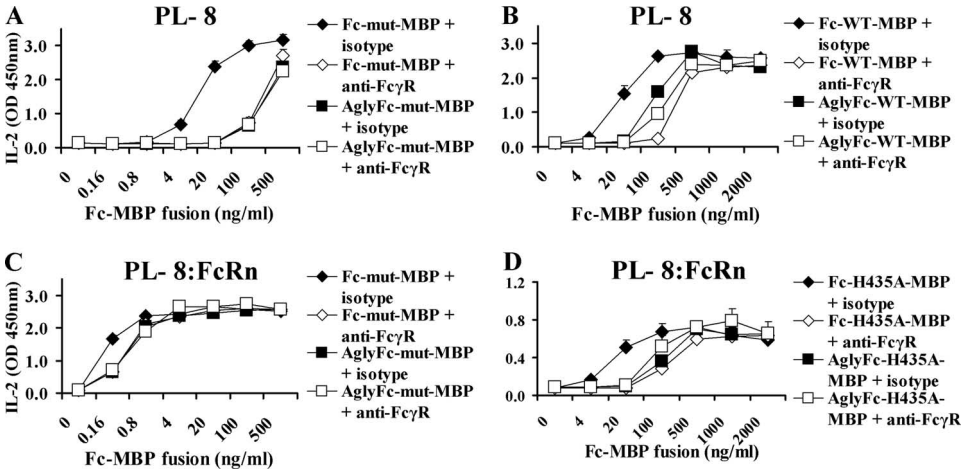

FIGURE 2. Role of FcγRs in responses of hybridoma 46 to Fc-MBP fusions. The data show IL-2 production following 24 h of incubation with Fc-MBP fusions in the presence of PL-8 (*A* and *B*) or PL-8:FcRn (*C* and *D*) cells as APCs with the addition of anti-FcγR Ab (2.4G2) or rat IgG2b (isotype-matched) control Ab. Error bars indicate SDs of triplicate samples. The data are representative of at least three independent experiments.

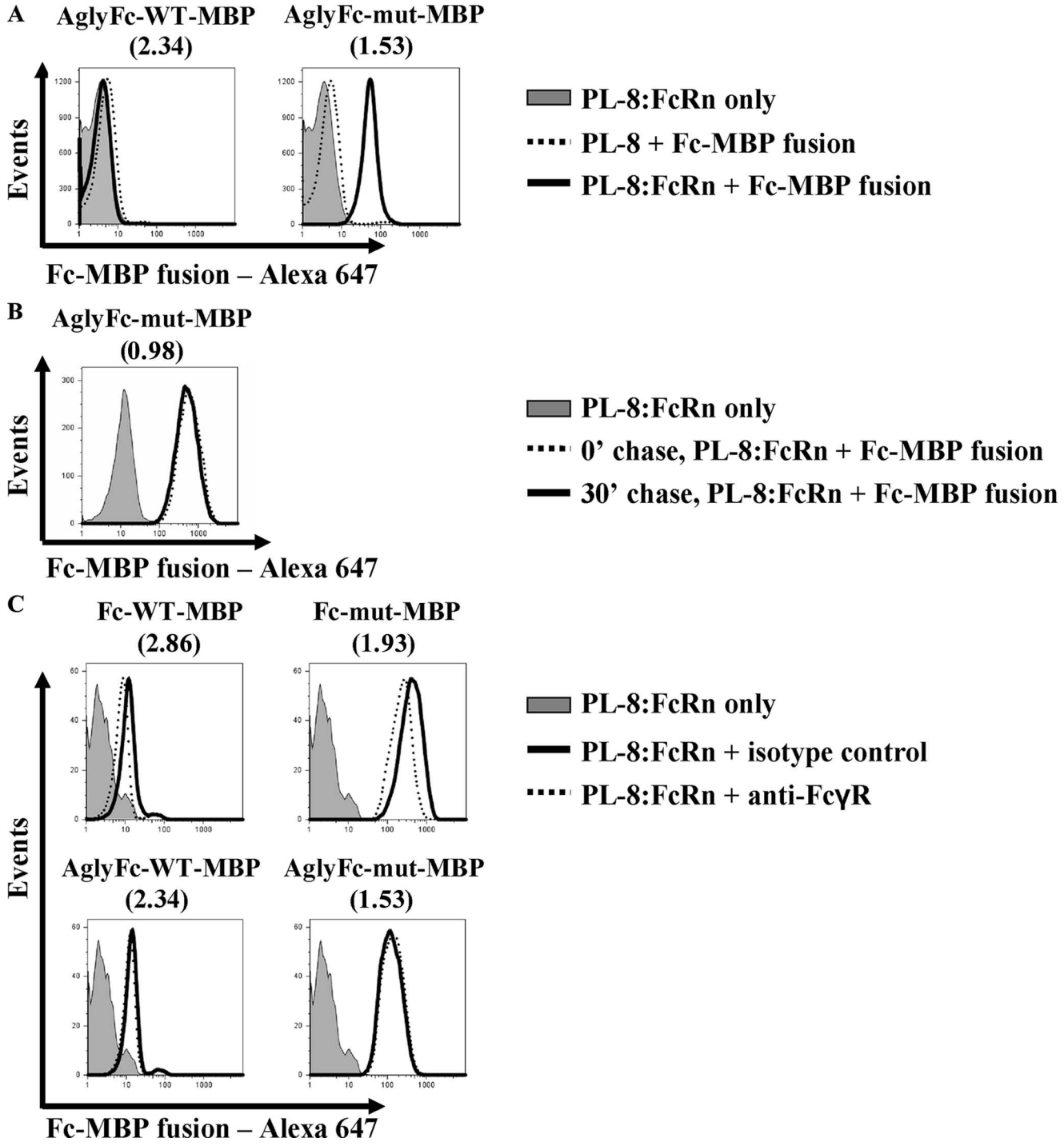

FIGURE 3. Flow cytometric analyses of uptake of Fc-MBP fusions by PL-8 or PL-8:FcRn cells. *A*, Uptake by PL-8 or PL-8:FcRn cells following incubation with Alexa 647-labeled Fc-MBP fusions (2 μg/ml) for 30 min at 37°C, washing, and analysis (no chase period). *B*, Uptake and retention of Fc-mut-MBP following a 30-min pulse with 2 μg/ml protein at 37°C followed by a 0- or 30-min chase period. *C*, PL-8:FcRn cells were preincubated with 5 μg/ml anti-FcγR Ab (2.4G2) or rat IgG2b followed by incubation with Alexa 647-labeled Fc-MBP fusion as in *A*. The degrees of labeling for each fluorescently labeled protein are indicated in parentheses. The data are representative of at least two independent experiments.

μg/ml (~33 nM) so that fluid phase uptake was low (42), allowing an assessment of enhanced uptake by receptor-mediated processes to be made. In some experiments, cells were also chased for 30 min after the pulse to analyze the retention of the recombinant proteins in cells (Fig. 3*B*). Consistent with their high affinities for FcRn at pH 6.0 and 7.4 (Table I), both glycosylated and aglycosylated Fc-mut-MBP fusions are taken up more efficiently by FcRn-expressing cells (PL-8:FcRn) relative to PL-8 cells (Fig. 3*A*). The levels of Fc-mut fusions associated with PL-8:FcRn cells do not change over a 30-min chase period (Fig. 3*B*; data not shown), indicating that these proteins are not recycled following uptake into cells. Additionally, the uptake of Fc-mut-MBP fusions in PL-8:FcRn cells was much greater than that of the corresponding Fc-WT-MBP fusions that do not bind detectably to FcRn at pH >7 (Fig. 3, *A* and *C*). Importantly, these differences were observed in cases where the degrees of labeling (molar ratio of Alexa 647

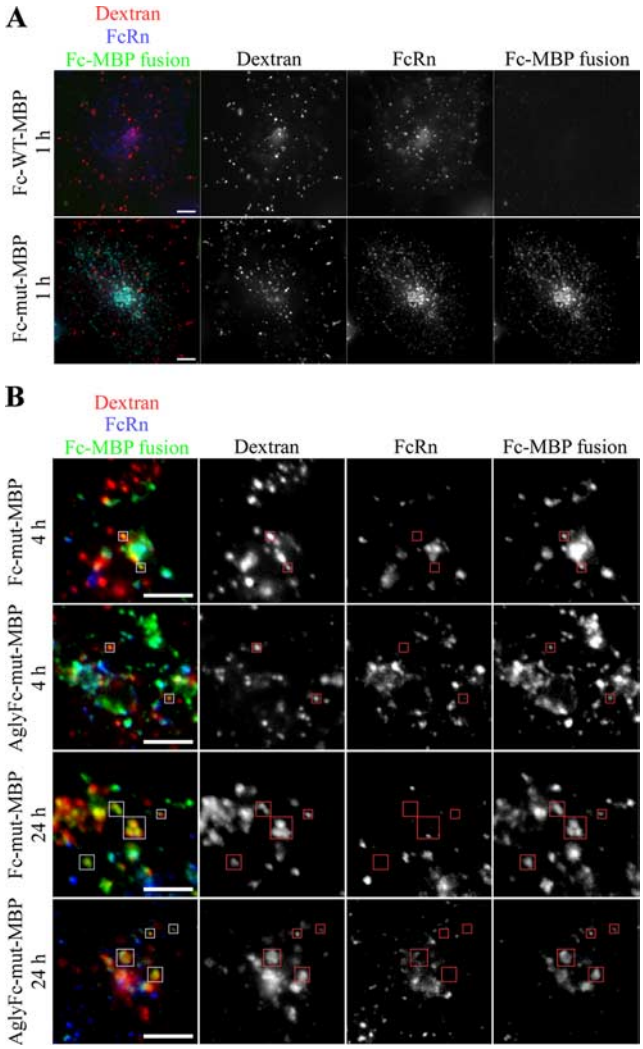

FIGURE 4. The intracellular trafficking of Fc-mut-MBP fusions following uptake into PL-8:FcRn cells. PL-8:FcRn cells were pulsed with Alexa 555-labeled dextran for 2 h, chased for 1 h, and incubated with 5 μg/ml Alexa 647-labeled Fc-MBP fusions for different times as indicated. *A*, Comparison of uptake by PL-8:FcRn cells of Fc-WT-MBP and Fc-mut-MBP following 1 h of incubation. The data show that Fc-mut-MBP is extensively colocalized with FcRn in endosomes, whereas the accumulation of Fc-WT-MBP is undetectable. Scale bars = 5 μm. *B*, White rectangles/squares show dextran$^+$ lysosomes with detectable Fc-mut-MBP or AglyFc-mut-MBP. The corresponding compartments in the single-color data are indicated by red rectangles/squares. In the overlay, FcRn-GFP is shown in blue, Alexa 555-labeled dextran in red, and Alexa 647-labeled Fc-MBP fusions in green. Scale bars = 5 μm.

dye to Fc-MBP fusion) of the Fc-mut-MBP fusions were lower than those for the corresponding Fc-WT-MBP proteins. The uptake of the glycosylated proteins was reduced slightly by preincubating the cells with anti-FcγRIIB/III (2.4G2) Ab, whereas FcγR blockade did not affect the accumulation of aglycosylated fusions (Fig. 3*C*).

Fc-mut-MBP fusions accumulate in lysosomes following uptake

Fluorescence microscopy analyses were conducted to determine the subcellular location of internalized Fc-mut-MBP over the course of 24 h (Fig. 4). These studies demonstrated that following 1 h of incubation, glycosylated and aglycosylated Fc-mut-MBP proteins were extensively colocalized with FcRn within PL-8:FcRn cells (Fig. 4*A* and data not shown). In contrast, the level of Fc-WT-MBP in cells was below the level of detection under the imaging conditions used (Fig. 4*A*). Following several hours of incubation, both glycosylated and aglycosylated Fc-mut-MBP proteins could be detected within lysosomes, and concomitant with a decrease in FcRn colocalization in endosomes, this lysosomal distribution increased up until 24 h postaddition (the last time point of imaging) (Fig. 4*B*). Recent studies have shown that FcRn can enter lysosomes in an invariant chain-dependent way in APCs (68) and/or on the constitutive degradation pathway (Z. Gan and E. S.Ward, unpublished observations). Thus, although Fc-mut-MBP fusions are most likely associated with FcRn during entry into lysosomes, FcRn-GFP cannot be detected in these compartments due to the sensitivity of enhanced GFP fluorescence to acidic pH, combined with the susceptibility of GFP to proteolytic degradation (69–71).

High-affinity binding to FcRn enhances responses of Ag-specific transgenic T cells and results in increased accumulation in different APC subsets

The ability of the different Fc-MBP proteins to stimulate Ag-specific naive T cells derived from mice that transgenically express the 1934.4 TCR (1934.4 tg mice; Ref. 45) was also investigated. Proliferation and IL-2 production in splenocyte cultures derived from these mice were assessed following addition of different concentrations of Fc-MBP fusions (Fig. 5). The pattern of stimulation was similar to that observed for PL-8:FcRn cells and T cell hybridomas (Fig. 1). Since splenocytes contain distinct APC subsets, we used flow cytometry to analyze the uptake of the Fc-MBP fusions by mDCs, macrophages, and B cells in freshly isolated splenocytes (Fig. 6*A*). Cells were pulsed with Alexa 647-labeled Fc-MBP fusions for 20 min in medium at 37°C, washed, and analyzed. These studies demonstrated that Fc-MBP fusions containing Fc-mut accumulate to higher levels in all APC subsets relative to their Fc-WT counterparts (Fig. 6*A*), with the uptake by macrophages being higher than that for DCs and B cells. In contrast, CD4$^+$ T cells that do not express FcRn or FcγRs (8, 17, 72) show similar, very low levels of (fluid phase) uptake of Fc-mut or Fc-WT fusions that are close to cellular autofluorescence levels

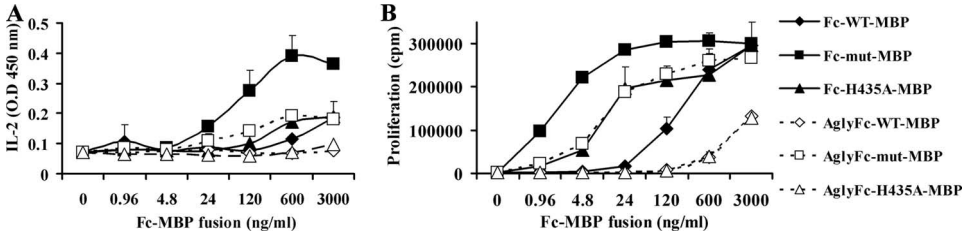

FIGURE 5. Responses of Ag-specific T cells from mice that transgenically express the 1934.4 TCR (45) to Fc-MBP fusions. *A* and *B*, Splenocytes from 1934.4 tg mice were incubated with Fc-MBP fusions, and IL-2 production (*A*) and proliferative responses (*B*) were assessed following 24 and 90 h of incubation, respectively. Error bars indicate SDs of duplicate samples. Data are representative of three independent experiments.

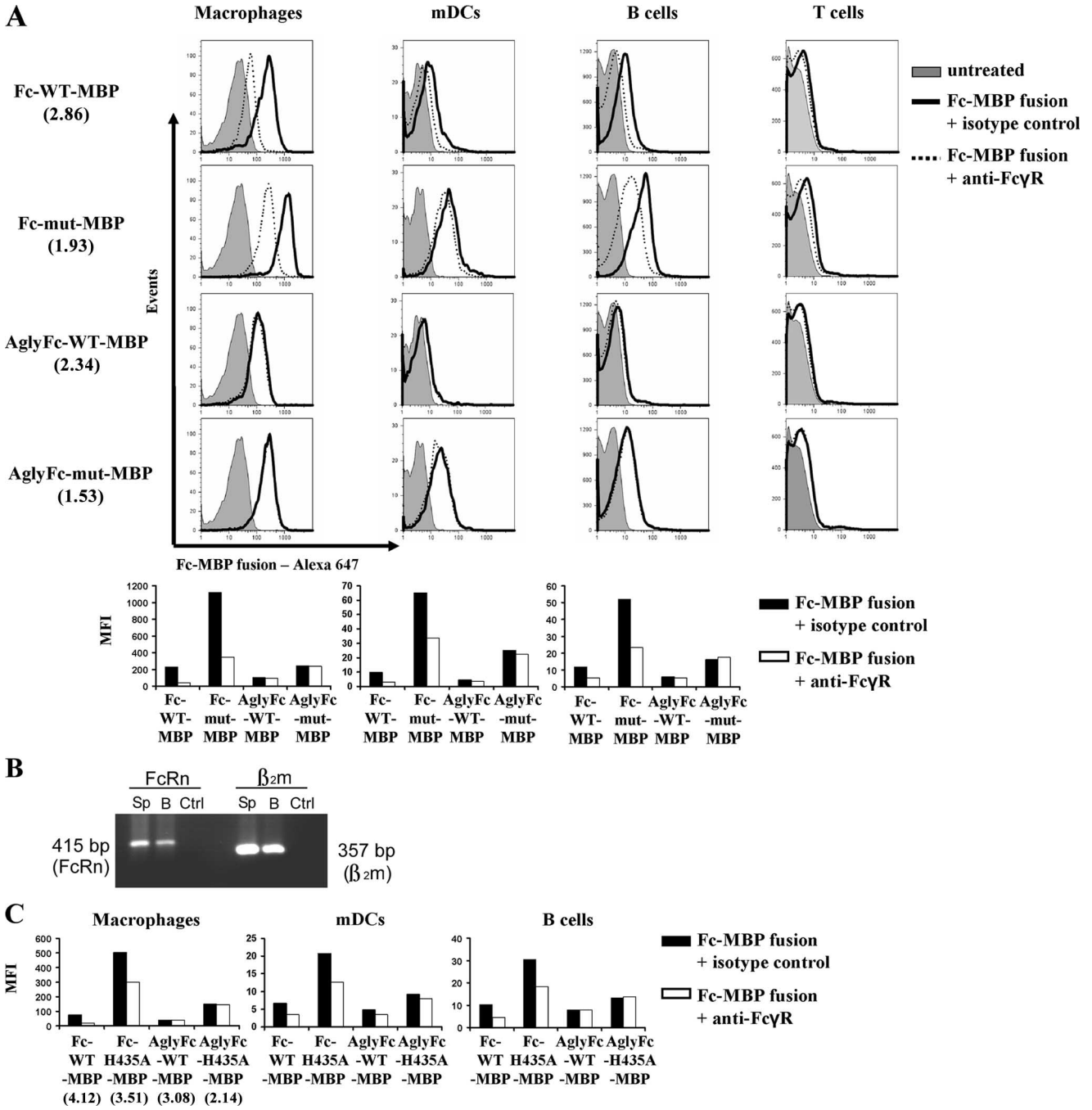

FIGURE 6. Uptake of Fc-MBP fusions by different APC populations and RT-PCR analysis of FcRn expression in sorted splenic B cells. *A*, Splenocytes of B10.PL mice were preincubated with 5 μg/ml anti-FcγR Ab (2.4G2) or rat IgG2b followed by incubation for 20 min with Alexa 647-labeled Fc-MBP fusions (5 μg/ml Fc-WT-MBP or Fc-mut-MBP fusions or their aglycosylated counterparts). The cells were then stained with fluorescently labeled Abs to identify each cell subset as described in *Materials and Methods*. Lower plots show the mean fluorescence intensities (MFIs) for cells treated with each Fc-MBP fusion following subtraction of MFIs for background autofluorescence. The degree of labeling for each fluorescently labeled protein is indicated in parentheses. *B*, RT-PCR analysis of FcRn α-chain expression in splenic B cells. $CD19^+B220^+$ B cells were sorted by flow cytometry, and RNA was isolated and used in RT-PCR with oligonucleotide primers specific for FcRn α-chain or β_2m. As a control, RT-PCR analyses were also conducted using RNA isolated from splenocytes (Sp) before sorting. Ctrl indicates negative control in which no cDNA was added to the PCR. *C*, Splenocytes were treated as in *A*, except that Fc-WT-MBP or Fc-H435A-MBP fusions and their aglycosylated counterparts were used. The degree of labeling for each fluorescently labeled protein is indicated in parentheses. Data are representative of two (*B*) or three (*A* and *C*) independent experiments.

(Fig. 6*A*). Although in earlier studies FcRn has been reported to not be expressed in primary B cells and B cell lines (8, 23, 72), RT-PCR analyses indicated the presence of FcRn in sorted primary B cells from B10.PL mice (Fig. 6*B*). Additionally, the presence of anti-FcγR Ab (2.4G2) reduced the uptake of glycosylated Fc-MBP fusions, whereas this blockade did not affect the accumulation of aglycosylated Fc-MBP fusions (Fig. 6*A*).

We also compared the uptake of Fc-WT-MBP and Fc-H435A-MBP fusions in different splenic APC subsets (Fig. 6*C*). The levels of cell-associated Fc-WT-MBP fusions were consistently lower than those of Fc-H435A-MBP fusions, and the addition of anti-FcγR Ab reduced the uptake of the glycosylated proteins but did not affect that of the aglycosylated counterparts. Importantly, the degree of labeling of the Fc-H435A-MBP fusions was lower than

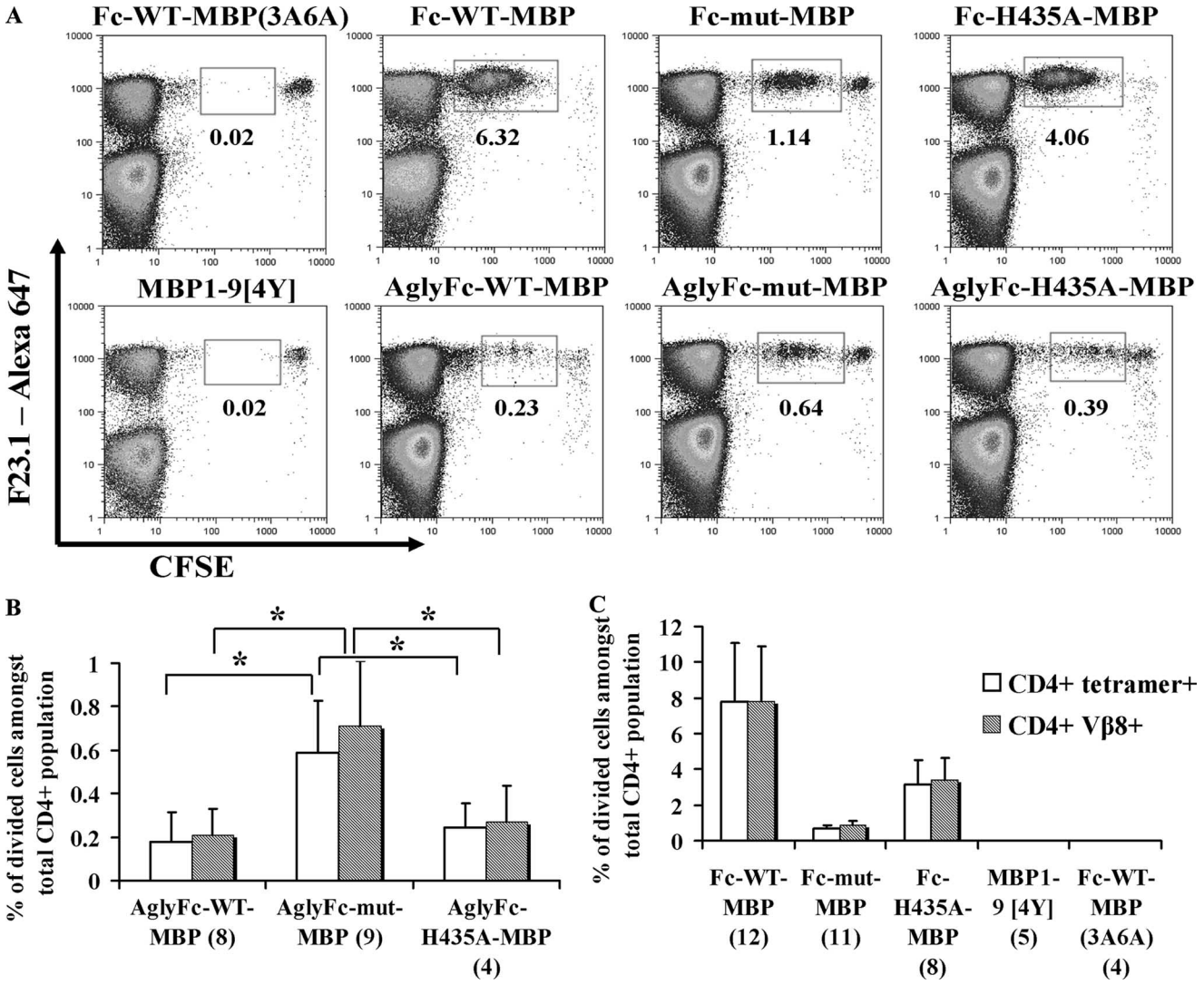

FIGURE 7. T cell proliferative responses following delivery of Fc-MBP fusions into B10.PL recipients. Splenocytes from 1934.4 tg mice were labeled with CFSE and transferred into B10.PL mice (2×10^6 $CD4^+$ cells/mouse). Mice were injected i.v. with 100 ng of each protein or 3.3 ng N-terminally acetylated MBP1–9[4Y] peptide. Three days later, splenocytes were harvested and stained with Alexa 647-labeled anti-Vβ8 (F23.1) and PE-labeled anti-CD4 Abs (*A*). Populations shown are gated on $CD4^+$ cells. Numbers represent the divided cells as a percentage of total $CD4^+$ cells. *B* and *C*, Mean percentages of divided V$\beta8^+$ or MBP1–9[4Y]:I-A^u $tetramer^+$ cells among the total $CD4^+$ cells for mice treated with aglycosylated (*B*) or glycosylated (*C*) Fc-MBP fusions. Total numbers of mice used in multiple different experiments are shown in parentheses. Error bars show SDs. In *B*, $*$ indicates groups that have significant differences in their mean percentages. Mean percentages for groups shown in *C* are all significantly different. Tests of significance were conducted using ANOVA with multiple comparisons at a confidence level of 95%.

that of the corresponding Fc-WT-MBP fusions, indicating that the lower levels of cell-associated Fc-WT-MBP fusions could not be accounted for by differences in fluorescent labeling (Fig. 6*C*). The lower accumulation of Fc-WT-MBP fusions in cells is consistent with FcRn-mediated recycling of WT Fc fragments (or IgGs) out of cells (35). In contrast, Fc-H435A-MBP fusions are not salvaged by FcRn into the recycling pathway following uptake (35).

Counterbalancing effects of FcRn targeting and in vivo persistence on T cell responses

We next analyzed the effects of the Fc-MBP fusions on T cell proliferative responses in vivo. CFSE-labeled MBP1–9:I-A^u-specific T cells derived from 1934.4 tg mice (45) were transferred into B10.PL recipients, followed by the i.v. injection of relatively low doses (100 ng, ~2 pmol) of glycosylated or aglycosylated proteins. Importantly, delivery of an amount of MBP1–9[4Y] peptide that is equivalent to that present in the injected Fc-MBP fusions (on a molar basis) induced no detectable T cell proliferation (Fig. 7*A*). Furthermore, the Ag specificity of the proliferative response was demonstrated by using an Fc-WT-MBP fusion (3A6A) in which the T cell contact residues in the MBP epitope had been mutated (Gln^3 to Ala, Pro^6 to Ala; Ref. 67) (Fig. 7*A*).

Comparison of the properties of the aglycosylated forms of Fc-WT-MBP, Fc-mut-MBP, and Fc-H435A-MBP that do not interact with FcγRs resulted in a similar ranking of stimulatory capacities to that observed in vitro, with aglycosylated Fc-mut-MBP being more effective than fusions containing Fc-WT or Fc-H435A (Fig. 7, *A* and *B*). In contrast, however, analyses of the glycosylated proteins resulted in distinct behavior to that observed in vitro: glycosylated Fc-WT-MBP induced substantially more Ag-specific T cell expansion relative to Fc-mut-MBP, with Fc-H435A-MBP inducing an intermediate level of proliferation (Fig. 7, *A* and *C*).

These observations raise the question as to why the relative activities of the glycosylated Fc-MBP fusions in stimulating T

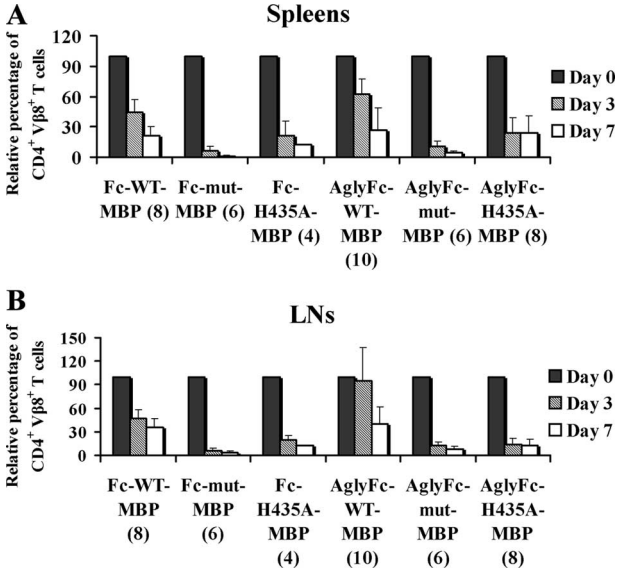

FIGURE 8. In vivo persistence of Ag following the delivery of Fc-MBP fusions. B10.PL mice were injected i.v. with 1 μg of the indicated proteins. One hour (Day 0), 3 days, or 7 days following Fc-MBP fusion delivery, mice were injected with CFSE-labeled splenocytes from 1934.4 tg mice or combined from 1934.4 tg and T/R$^+$ tg mice (2×10^6 CD4$^+$ cells/mouse). Three days later, splenocytes and lymph node cells were stained as in Fig. 7. Proliferative responses for each protein were normalized to those observed for mice in which Fc-MBP fusion and CFSE-labeled cells were transferred within 1 h of each other (Day 0). Injections of Fc-MBP fusions were staggered so that mice in each experiment received transferred, CFSE-labeled cells from the same mixture. Total numbers of mice used in multiple different experiments (using two mice per protein per time point) are shown in parentheses. The data shown represent mean values with error bars indicating SDs. At day 3, significant differences were observed for all pairwise comparisons of glycosylated and aglycosylated Fc-WT-MBP fusions vs corresponding Fc-mut-MBP or Fc-H435A-MBP fusions (using ANOVA at a confidence level of 95%). At day 7, the following comparisons showed significant differences (using ANOVA at a confidence level of 95%): Fc-WT-MBP vs Fc-mut-MBP (spleen and lymph node) and Fc-WT-MBP vs Fc-H435A-MBP (lymph node).

cells are different in vivo and in vitro. An obvious distinction between these analyses is that the half-life and distribution of Fc-MBP fusions will have an impact during in vivo studies. The different binding properties of Fc-WT-MBP, Fc-mut-MBP, and Fc-H435A-MBP for FcRn are expected to result in variations in longevity in vivo (27–30). We therefore analyzed the persistence of functional Ag derived from each type of protein by determining the proliferative responses of CFSE-labeled, Ag-specific T cells that were transferred into B10.PL recipients at different times following delivery of the Fc-MBP fusions. These studies indicated that cognate Ag derived from Fc-WT-MBP persisted for longer than that generated from Fc-mut-MBP or Fc-H435A-MBP, and this was observed for both glycosylated and aglycosylated proteins (Fig. 8). Additionally, Fc-MBP fusions containing Fc-mut showed a trend toward more rapid clearance than those comprising Fc-H435A, although the differences were not all significant (at a 95% confidence level). This is consistent with our earlier data indicating that loss of pH-dependent binding to FcRn results in enhanced clearance (29, 30).

Discussion

The expression of the MHC class I-related receptor, FcRn, in professional APCs (23) raises questions concerning its functional relevance. Additionally, the location of this receptor in the endosomal pathway (35) suggests that it might be a useful target for enhancing Ag delivery. In the present study we have therefore analyzed the effect of targeting Ag to the FcRn trafficking pathway on cognate T cell responses. This has been achieved by using recombinant Fc-MBP fusions that differ in their binding properties for FcRn. In addition to a wild-type mouse IgG1-derived Fc fragment, we have used a mutated variant (Fc-mut) that binds with substantially increased affinity for FcRn in the pH range 6.0–7.4 and an Fc mutant (H435A) that does not bind detectably to FcRn. These Fc fragments not only have different FcRn targeting abilities, but also have distinct in vivo half-lives, allowing the impact of Ag persistence on T cell responses to be evaluated. Additionally, to probe the relative contributions of FcRn and FcγRs to Ag delivery, the Fc fragments have been used in both glycosylated and aglycosylated forms that do and do not, respectively, interact with FcγRs.

In vitro, Fc-mut-MBP fusions are more effective than their counterparts containing Fc-WT or Fc-H435A in stimulating Ag-specific T cells when FcRn-expressing APCs are used. This difference is observed with both glycosylated and aglycosylated proteins. These observations can be explained by the high efficiency of uptake of Fc-mut by receptor-mediated processes together with accumulation in the endolysosomal system of FcRn-expressing cells (this study and Ref. 42). By contrast with the in vitro analyses, however, glycosylated Fc-WT-MBP is more effective compared with its counterpart containing Fc-mut in inducing the proliferation of transferred Ag-specific T cells in mice. The higher in vivo stimulatory capacity of glycosylated Fc-WT-MBP relative to Fc-mut-MBP can be attributed to several factors. First, delivery of the Fc-WT-MBP fusion in vivo results in greater persistence of Ag (peptide:I-A^u) complexes relative to Fc-mut-MBP, which, consistent with its FcRn interaction properties, is cleared rapidly (29, 30). Second, FcRn is expressed in multiple other cell types, including those of endothelial and epithelial origin (11, 13, 18–20). This is expected to result in dilution of the effective concentration that is available in vivo for uptake of Fc-mut-MBP by APCs such as DCs. The enhancement of in vivo proliferative responses by FcγR interactions with the Fc-MBP fusions is revealed by analyses of their aglycosylated counterparts, which show that Fc-WT-MBP and Fc-H435A-MBP, in particular, are markedly reduced in activity when binding to FcγRs is ablated. Consequently, when aglycosylated Fc-MBP fusions are delivered at a relatively low dose of ~2 pmol/mouse, the increase in uptake into (Ag-presenting) cells due to high-affinity binding to FcRn by Fc-mut-MBP becomes apparent. This results in greater T cell expansion for aglycosylated Fc-mut-MBP relative to analogous Fc-MBP fusions containing Fc-WT or Fc-H435A that both rely on fluid phase uptake for entry into cells.

The shorter in vivo persistence of Fc-mut illustrates the trade-off that is observed when protein engineering is used to generate Fc fragments (or IgGs) that can efficiently target FcRn. Effective uptake and retention in FcRn$^+$ cells requires substantial increases in affinity of an Fc fragment for FcRn binding in the pH range 6.0–7.4, and such Fc fragments/IgGs (or Abdegs) can compete with endogenous IgGs for FcRn binding (30, 42). However, loss of the marked pH dependence of an FcRn-Fc interaction results in reduced in vivo persistence (29, 30, 42). The short in vivo half-lives of such IgGs/Fc fragments most likely result from retention within cells due to reduced exocytic release, combined with their FcRn-directed trafficking during the constitutive degradation of this Fc receptor and/or invariant chain-directed delivery of FcRn to lysosomes (Ref. 68 and Z. Gan and E. S. Ward, unpublished). Consequently, Fc fragments that are potent, FcRn-mediated Ag delivery reagents have short in vivo half-lives. The dual and opposing effects of increasing FcRn binding vs in vivo half-life become apparent during analyses in mice when Fc fusions that can bind to

FcγRs are used, with the consequence that in vivo persistence is a key determinant of T cell proliferative responses. However, when FcγR binding is ablated, FcRn targeting by an Abdeg becomes dominant and, at the relatively low doses used in this study, the short-lived Fc-mut-MBP is the most effective protein in inducing proliferation in vivo. The role of FcγRs in enhancing immune responses is complex and can occur through both increased Ag uptake and activation of DCs (21, 73, 74). Given that we are using mouse IgG1-derived Fc fragments that in the steady-state (noninflammatory) would be expected to result in a bias toward inhibitory signaling (75), the enhancement of proliferation in response to glycosylated Fc-MBP fusions is expected to be primarily due to increased internalization into cells rather than signaling effects through FcγRs.

The use of I-A^u-expressing B lymphoblastoid (PL-8) cells that are transfected to express mouse FcRn provides us with a useful system to assess the impact of FcRn expression on Ag presentation. However, DCs are the initiators of immune responses in vivo (76), and there are differences between Ag presentation, processing, and trafficking in B cells and DCs (71, 77). Additionally, PL-8 cells do not express endogenous FcRn. Importantly, the similar rankings of activities of different Fc-MBP fusions in in vitro Ag presentation assays using splenocytes or PL-8:FcRn cells indicate that our data with PL-8 cells can be correlated with behavior in APCs that have endogenous FcRn expression. However, we cannot exclude the possibility that there might be differences in intracellular trafficking that are not detectable in our assays.

Our data also have relevance to understanding how FcRn might impact Ag presentation pathways when naturally occurring Abs are bound to Ag. Although we cannot extrapolate the results from the current study to immune complexes, our observations suggest that monomeric IgG-Ag complexes can evade the degradative compartments that play an important role in Ag presentation by being recycled out of FcRn-expressing cells. Specifically, we observe that Fc-WT-MBP fusions accumulate to lower levels in cells and are less effective in stimulating cognate T cells in vitro with FcRn-expressing APCs than their counterparts containing H435A that do not bind to FcRn. The behavior of monomeric IgG-Ag complexes contrasts with that described for immune complexes in a recent study (72), in which such complexes were directed into lysosomes following uptake into cells. These observations indicate that FcRn crosslinking enhances lysosomal delivery. In this context, some epitopes can be processed and loaded onto MHC class II molecules during endosomal recycling (78–82). For such epitopes, FcRn-mediated "diversion" of monomeric IgG-Ag complexes away from degradation and into the recycling pathway might therefore not reduce Ag presentation unless FcRn binding sterically inhibits Ag degradation/loading onto MHC class II. The impact of FcRn will therefore depend on the processing requirements of the specific epitope and whether it remains stably bound to cognate IgG at the slightly acidic pH of the endosomal recycling system. Although MBP-derived epitopes have been shown to be loaded onto recycling HLA-DR molecules (78), our present data indicating that FcRn-mediated recycling of Fc-WT-MBP fusions can decrease Ag presentation in vitro suggest that this is not the major pathway for the loading of MBP1–9[4Y] onto I-A^u. How such recycling impacts in vivo T cell responses is made more complex by the interplay of the influence of FcRn binding properties on intracellular trafficking pathways and in vivo persistence.

An unexpected outcome of the present study is that, although FcRn has been shown to not be expressed by in vitro B cell lines of both human and mouse origin (8, 23), this receptor is present in splenic B cells isolated directly ex vivo. FcRn expression can therefore be extended to this class of professional APCs, and this raises questions concerning its function. In addition to providing an additional depot of hematopoietic cells that might regulate IgG levels in vivo (83), it is possible that this receptor performs functions in this cell type that are related to Ag presentation and/or the intracellular trafficking of IgG. However, given the central role of DCs in initiating immune responses (76), it is likely that these cells are the relevant APCs in our short-term proliferation assays in vivo.

Taken together, we demonstrate that targeting FcRn with high-affinity, engineered Fc-MBP fusions can elicit T cell responses both in vitro and in vivo. This broadens the previously defined roles of FcRn to encompass a function in the delivery of Ag to endolysosomal compartments in APCs. FcRn might therefore be a useful target for Ag loading, particularly when FcγR-mediated effects are to be avoided to minimize DC activation in the steady-state (2, 84). Future studies will be directed toward understanding the factors that lead to immune activation vs tolerance induction using these targeting approaches.

Acknowledgments

We thank Paula Marcos Mondejar and Tuyetanh Nguyen for assistance with the generation and analysis of recombinant proteins. We are grateful to Hector Perez Montoyo and Carlos Vaccaro for expert assistance, and to Silvia Pastor for providing hybridoma 46. We are also indebted to Dr. Joan Reisch and Angie Mobley for assistance with statistical analyses and FACS, respectively.

Disclosures

The authors have no financial conflicts of interest.

References

1. Bonifaz, L. C., D. P. Bonnyay, A. Charalambous, D. I. Darguste, S. Fujii, H. Soares, M. K. Brimnes, B. Moltedo, T. M. Moran, and R. M. Steinman. 2004. In vivo targeting of antigens to maturing dendritic cells via the DEC-205 receptor improves T cell vaccination. *J. Exp. Med.* 199: 815–824.
2. Hawiger, D., K. Inaba, Y. Dorsett, M. Guo, K. Mahnke, M. Rivera, J. V. Ravetch, R. M. Steinman, and M. C. Nussenzweig. 2001. Dendritic cells induce peripheral T cell unresponsiveness under steady state conditions in vivo. *J. Exp. Med.* 194: 769–779.
3. He, L. Z., A. Crocker, J. Lee, J. Mendoza-Ramirez, X. T. Wang, L. A. Vitale, T. O'Neill, C. Petromilli, H. F. Zhang, J. Lopez, et al. 2007. Antigenic targeting of the human mannose receptor induces tumor immunity. *J. Immunol.* 178: 6259–6267.
4. Zaliauskiene, L., S. Kang, K. Sparks, K. R. Zinn, L. M. Schwiebert, C. T. Weaver, and J. F. Collawn. 2002. Enhancement of MHC class II-restricted responses by receptor-mediated uptake of peptide antigens. *J. Immunol.* 169: 2337–2345.
5. Trombetta, E. S., and I. Mellman. 2005. Cell biology of antigen processing in vitro and in vivo. *Annu. Rev. Immunol.* 23: 975–1028.
6. Vely, F., and E. Vivier. 1997. Conservation of structural features reveals the existence of a large family of inhibitory cell surface receptors and noninhibitory/activatory counterparts. *J. Immunol.* 159: 2075–2077.
7. Ravetch, J. V., and S. Bolland. 2001. IgG Fc receptors. *Annu. Rev. Immunol.* 19: 275–290.
8. Ghetie, V., J. G. Hubbard, J. K. Kim, M. F. Tsen, Y. Lee, and E. S. Ward. 1996. Abnormally short serum half-lives of IgG in β_2-microglobulin-deficient mice. *Eur. J. Immunol.* 26: 690–696.
9. Junghans, R. P., and C. L. Anderson. 1996. The protection receptor for IgG catabolism is the β_2-microglobulin-containing neonatal intestinal transport receptor. *Proc. Natl. Acad. Sci. USA* 93: 5512–5516.
10. Israel, E. J., D. F. Wilsker, K. C. Hayes, D. Schoenfeld, and N. E. Simister. 1996. Increased clearance of IgG in mice that lack β_2-microglobulin: possible protective role of FcRn. *Immunology* 89: 573–578.
11. Dickinson, B. L., K. Badizadegan, Z. Wu, J. C. Ahouse, X. Zhu, N. E. Simister, R. S. Blumberg, and W. I. Lencer. 1999. Bidirectional FcRn-dependent IgG transport in a polarized human intestinal epithelial cell line. *J. Clin. Invest.* 104: 903–911.
12. McCarthy, K. M., Y. Yoong, and N. E. Simister. 2000. Bidirectional transcytosis of IgG by the rat neonatal Fc receptor expressed in a rat kidney cell line: a system to study protein transport across epithelia. *J. Cell Sci.* 113: 1277–1285.
13. Spiekermann, G. M., P. W. Finn, E. S. Ward, J. Dumont, B. L. Dickinson, R. S. Blumberg, and W. I. Lencer. 2002. Receptor-mediated immunoglobulin G transport across mucosal barriers in adult life: functional expression of FcRn in the mammalian lung. *J. Exp. Med.* 196: 303–310.

14. Claypool, S. M., B. L. Dickinson, J. S. Wagner, F.-E. Johansen, N. Venu, J. A. Borawski, W. I. Lencer, and R. S. Blumberg. 2004. Bidirectional transepithelial IgG transport by a strongly polarized basolateral membrane Fcγ receptor. *Mol. Biol. Cell* 15: 1746–1759.
15. Hirano, M., R. S. Davis, W. D. Fine, S. Nakamura, K. Shimizu, H. Yagi, K. Kato, R. P. Stephan, and M. D. Cooper. 2007. IgE^b immune complexes activate macrophages through FcγRIV binding. *Nat. Immunol.* 8: 762–771.
16. Amigorena, S., and C. Bonnerot. 1999. Fc receptor signaling and trafficking: a connection for antigen processing. *Immunol. Rev.* 172: 279–284.
17. Nimmerjahn, F., and J. V. Ravetch. 2006. Fcγ receptors: old friends and new family members. *Immunity* 24: 19–28.
18. Borvak, J., J. Richardson, C. Medesan, F. Antohe, C. Radu, M. Simionescu, V. Ghetie, and E. S. Ward. 1998. Functional expression of the MHC class I-related receptor, FcRn, in endothelial cells of mice. *Int. Immunol.* 10: 1289–1298.
19. Kobayashi, N., Y. Suzuki, T. Tsuge, K. Okumura, C. Ra, and Y. Tomino. 2002. FcRn-mediated transcytosis of immunoglobulin G in human renal proximal tubular epithelial cells. *Am. J. Physiol.* 282: F358–F365.
20. Ghetie, V., and E. S. Ward. 2000. Multiple roles for the major histocompatibility complex class I-related receptor FcRn. *Annu. Rev. Immunol.* 18: 739–766.
21. Kalergis, A. M., and J. V. Ravetch. 2002. Inducing tumor immunity through the selective engagement of activating Fcγ receptors on dendritic cells. *J. Exp. Med.* 195: 1653–1659.
22. Desai, D. D., S. O. Harbers, M. Flores, L. Colonna, M. P. Downie, A. Bergtold, S. Jung, and R. Clynes. 2007. Fcγ receptor IIB on dendritic cells enforces peripheral tolerance by inhibiting effector T cell responses. *J. Immunol.* 178: 6217–6226.
23. Zhu, X., G. Meng, B. L. Dickinson, X. Li, E. Mizoguchi, L. Miao, Y. Wang, C. Robert, B. Wu, P. D. Smith, et al. 2001. MHC class I-related neonatal Fc receptor for IgG is functionally expressed in monocytes, intestinal macrophages, and dendritic cells. *J. Immunol.* 166: 3266–3276.
24. Bonnerot, C., V. Briken, V. Brachet, D. Lankar, S. Cassard, B. Jabri, and S. Amigorena. 1998. Syk protein tyrosine kinase regulates Fc receptor γ-chain-mediated transport to lysosomes. *EMBO J.* 17: 4606–4616.
25. Amigorena, S., D. Lankar, V. Briken, L. Gapin, M. Viguier, and C. Bonnerot. 1998. Type II and III receptors for immunoglobulin G (IgG) control the presentation of different T cell epitopes from single IgG-complexed antigens. *J. Exp. Med.* 187: 505–515.
26. Phillips, W. J., D. J. Smith, C. A. Bona, A. Bot, and H. Zaghouani. 2005. Recombinant immunoglobulin-based epitope delivery: a novel class of autoimmune regulators. *Int. Rev. Immunol.* 24: 501–517.
27. Medesan, C., D. Matesoi, C. Radu, V. Ghetie, and E. S. Ward. 1997. Delineation of the amino acid residues involved in transcytosis and catabolism of mouse IgG1. *J. Immunol.* 158: 2211–2217.
28. Ghetie, V., S. Popov, J. Borvak, C. Radu, D. Matesoi, C. Medesan, R. J. Ober, and E. S. Ward. 1997. Increasing the serum persistence of an IgG fragment by random mutagenesis. *Nat. Biotechnol.* 15: 637–640.
29. Dall'Acqua, W., R. M. Woods, E. S. Ward, S. R. Palaszynski, N. K. Patel, Y. A. Brewah, H. Wu, P. A. Kiener, and S. Langermann. 2002. Increasing the affinity of a human IgG1 to the neonatal Fc receptor: biological consequences. *J. Immunol.* 169: 5171–5180.
30. Vaccaro, C., R. Bawdon, S. Wanjie, R. J. Ober, and E. S. Ward. 2006. Divergent activities of an engineered antibody in murine and human systems have implications for therapeutic antibodies. *Proc. Natl. Acad. Sci. USA* 103: 18709–18714.
31. Rodewald, R. 1976. pH-dependent binding of immunoglobulins to intestinal cells of the neonatal rat. *J. Cell Biol.* 71: 666–669.
32. Wallace, K. H., and A. R. Rees. 1980. Studies on the immunoglobulin-G Fc-fragment receptor from neonatal rat small intestine. *Biochem. J.* 188: 9–16.
33. Popov, S., J. G. Hubbard, J. Kim, B. Ober, V. Ghetie, and E. S. Ward. 1996. The stoichiometry and affinity of the interaction of murine Fc fragments with the MHC class I-related receptor, FcRn. *Mol. Immunol.* 33: 521–530.
34. Raghavan, M., V. R. Bonagura, S. L. Morrison, and P. J. Bjorkman. 1995. Analysis of the pH dependence of the neonatal Fc receptor/immunoglobulin G interaction using antibody and receptor variants. *Biochemistry* 34: 14649–14657.
35. Ober, R. J., C. Martinez, C. Vaccaro, J. Zhou, and E. S. Ward. 2004. Visualizing the site and dynamics of IgG salvage by the MHC class I-related receptor, FcRn. *J. Immunol.* 172: 2021–2029.
36. Bergtold, A., D. D. Desai, A. Gavhane, and R. Clynes. 2005. Cell surface recycling of internalized antigen permits dendritic cell priming of B cells. *Immunity* 23: 503–514.
37. Duncan, A. R., J. M. Woof, L. J. Partridge, D. R. Burton, and G. Winter. 1988. Localization of the binding site for the human high-affinity Fc receptor on IgG. *Nature* 332: 563–564.
38. Kim, J. K., M. F. Tsen, V. Ghetie, and E. S. Ward. 1994. Localization of the site of the murine IgG1 molecule that is involved in binding to the murine intestinal Fc receptor. *Eur. J. Immunol.* 24: 2429–2434.
39. Martin, W. L., A. P. J. West, L. Gan, and P. J. Bjorkman. 2001. Crystal structure at 2.8 Å of an FcRn/heterodimeric Fc complex: mechanism of pH dependent binding. *Mol. Cell.* 7: 867–877.
40. Wines, B. D., M. S. Powell, P. W. Parren, N. Barnes, and P. M. Hogarth. 2000. The IgG Fc contains distinct Fc receptor (FcR) binding sites: the leukocyte receptors FcγRI and FcγRIIa bind to a region in the Fc distinct from that recognized by neonatal FcR and protein A. *J. Immunol.* 164: 5313–5318.
41. Shields, R. L., A. K. Namenuk, K. Hong, Y. G. Meng, J. Rae, J. Briggs, D. Xie, J. Lai, A. Stadlen, B. Li, et al. 2001. High resolution mapping of the binding site on human IgG1 for FcγRI, FcγRII, FcγRIII, and FcRn and design of IgG1 variants with improved binding to the FcγR. *J. Biol. Chem.* 276: 6591–6604.
42. Vaccaro, C., J. Zhou, R. J. Ober, and E. S. Ward. 2005. Engineering the Fc region of immunoglobulin G to modulate in vivo antibody levels. *Nat. Biotechnol.* 23: 1283–1288.
43. Ober, R. J., C. Martinez, X. Lai, J. Zhou, and E. S. Ward. 2004. Exocytosis of IgG as mediated by the receptor, FcRn: an analysis at the single-molecule level. *Proc. Natl. Acad. Sci. USA* 101: 11076–11081.
44. Zamvil, S. S., D. J. Mitchell, A. C. Moore, K. Kitamura, L. Steinman, and J. B. Rothbard. 1986. T-cell epitope of the autoantigen myelin basic protein that induces encephalomyelitis. *Nature* 324: 258–260.
45. Pearson, C. I. W., and H. O. McDevitt. 1997. Induction of apoptosis and T helper 2 (Th2) responses correlates with peptide affinity for the major histocompatibility complex in self-reactive T cell receptor transgenic mice. *J. Exp. Med.* 185: 583–599.
46. Lafaille, J. J., K. Nagashima, M. Katsuki, and S. Tonegawa. 1994. High incidence of spontaneous autoimmune encephalomyelitis in immunodeficient anti-myelin basic protein T cell receptor transgenic mice. *Cell* 78: 399–408.
47. Urban, J. L., V. Kumar, D. H. Kono, C. Gomez, S. J. Horvath, J. Clayton, D. G. Ando, E. E. Sercarz, and L. Hood. 1988. Restricted use of T cell receptor V genes in murine autoimmune encephalomyelitis raises possibilities for antibody therapy. *Cell* 54: 577–592.
48. Huang, J. C., M. Han, A. Minguela, S. Pastor, A. Qadri, and E. S. Ward. 2003. T cell recognition of distinct peptide:I-A^u conformers in murine experimental autoimmune encephalomyelitis. *J. Immunol.* 171: 2467–2477.
49. Wraith, D. C., D. E. Smilek, D. J. Mitchell, L. Steinman, and H. O. McDevitt. 1989. Antigen recognition in autoimmune encephalomyelitis and the potential for peptide-mediated immunotherapy. *Cell* 59: 247–255.
50. Kim, J. K., M. F. Tsen, V. Ghetie, and E. S. Ward. 1994. Identifying amino acid residues that influence plasma clearance of murine IgG1 fragments by site-directed mutagenesis. *Eur. J. Immunol.* 24: 542–548.
51. Horton, R. M., H. D. Hunt, S. N. Ho, J. K. Pullen, and L. R. Pease. 1989. Engineering hybrid genes without the use of restriction enzymes: gene splicing by overlap extension. *Gene* 77: 61–68.
52. Kim, J. K., M. Firan, C. G. Radu, C. H. Kim, V. Ghetie, and E. S. Ward. 1999. Mapping the site on human IgG for binding of the MHC class I-related receptor, FcRn. *Eur. J. Immunol.* 29: 2819–2825.
53. Zhou, J., J. E. Johnson, V. Ghetie, R. J. Ober, and Ward, E. S. 2003. Generation of mutated variants of the human form of the MHC class I-related receptor, FcRn, with increased affinity for mouse immunoglobulin G. *J. Mol. Biol.* 332: 901–913.
54. Zhou, J., F. Mateos, R. J. Ober, and E. S. Ward. 2005. Conferring the binding properties of the mouse MHC class I-related receptor, FcRn, onto the human ortholog by sequential rounds of site-directed mutagenesis. *J. Mol. Biol.* 345: 1071–1081.
55. Radu, C. G., S. M. Anderton, M. Firan, D. C. Wraith, and E. S. Ward. 2000. Detection of autoreactive T cells in H-2^u mice using peptide-MHC multimers. *Int. Immunol.* 12: 1553–1560.
56. Minguela, A., S. Pastor, W. Mi, J. A. Richardson, and E. S. Ward. 2007. Feedback regulation of murine autoimmunity via dominant anti-inflammatory effects of interferon γ. *J. Immunol.* 178: 134–144.
57. Ahouse, J. J., C. L. Hagerman, P. Mittal, D. J. Gilbert, N. G. Copeland, N. A. Jenkins, and N. E. Simister. 1993. Mouse MHC class I-like Fc receptor encoded outside the MHC. *J. Immunol.* 151: 6076–6088.
58. Mason, K., D. W. Denney, Jr., and H. M. McConnell. 1995. Myelin basic protein peptide complexes with the class II molecules I-A^u and I-A^k form and dissociate rapidly at neutral pH. *J. Immunol.* 154: 5216–5227.
59. Liu, G. Y., P. J. Fairchild, R. M. Smith, J. R. Prowle, D. Kioussis, and D. C. Wraith. 1995. Low avidity recognition of self-antigen by T cells permits escape from central tolerance. *Immunity* 3: 407–415.
60. He, X., C. Radu, J. Sidney, A. Sette, E. S. Ward, and K. C. Garcia. 2002. Structural snapshot of aberrant antigen presentation linked to autoimmunity: the immunodominant epitope of MBP complexed with I-A^u. *Immunity* 17: 83–94.
61. Wawrzynczak, E. J., A. J. Cumber, G. D. Parnell, P. T. Jones, and G. Winter. 1992. Blood clearance in the rat of a recombinant mouse monoclonal antibody lacking the N-linked oligosaccharide side chains of the C_H2 domains. *Mol. Immunol.* 29: 213–220.
62. Tao, M. H., and S. L. Morrison. 1989. Studies of aglycosylated chimeric mouse-human IgG: role of carbohydrate in the structure and effector functions mediated by the human IgG constant region. *J. Immunol.* 143: 2595–2601.
63. Nimmerjahn, F., P. Bruhns, K. Horiuchi, and J. V. Ravetch. 2005. FcγRIV: a novel FcR with distinct IgG subclass specificity. *Immunity* 23: 41–51.
64. Antoniou, A. N., S. L. Blackwood, D. Mazzeo, and C. Watts. 2000. Control of antigen presentation by a single protease cleavage site. *Immunity* 12: 319–398.
65. Harbers, S. O., A. Crocker, G. Catalano, V. D'Agati, S. Jung, D. D. Desai, and R. Clynes. 2007. Antibody-enhanced cross-presentation of self antigen breaks T cell tolerance. *J. Clin. Invest.* 117: 1361–1369.
66. Wraith, D. C., D. E. Smilek, and S. Webb. 1992. MHC-binding peptides for immunotherapy of experimental autoimmune disease. *J. Autoimmun.* 5 (*Suppl.* A): 103–113.
67. Anderton, S. M., S. P. Manickasingham, C. Burkhart, T. A. Luckcuck, S. J. Holland, A. G. Lamont, and D. C. Wraith. 1998. Fine specificity of the myelin-reactive T cell repertoire: implications for TCR antagonism in autoimmunity. *J. Immunol.* 161: 3357–3364.
68. Ye, L., X. Liu, S. N. Rout, Z. Li, Y. Yan, L. Lu, T. Kamala, N. K. Nanda, W. Song, S. K. Samal, and X. Zhu. 2008. The MHC class II-associated invariant chain interacts with the neonatal Fcγ receptor and modulates its trafficking to endosomal/lysosomal compartments. *J. Immunol.* 181: 2572–2585.

69. Patterson, G. H., S. M. Knobel, W. D. Sharif, S. R. Kain, and D. W. Piston. 1997. Use of the green fluorescent protein and its mutants in quantitative fluorescence microscopy. *Biophys. J.* 73: 2782–2790.
70. Katayama, H., A. Yamamoto, N. Mizushima, T. Yoshimori, and A. Miyawaki. 2008. GFP-like proteins stably accumulate in lysosomes. *Cell Struct. Funct.* 33: 1–12.
71. Delamarre, L., M. Pack, H. Chang, I. Mellman, and E. S. Trombetta. 2005. Differential lysosomal proteolysis in antigen-presenting cells determines antigen fate. *Science* 307: 1630–1634.
72. Qiao, S. W., K. Kobayashi, F. E. Johansen, L. M. Sollid, J. T. Andersen, E. Milford, D. C. Roopenian, W. I. Lencer, and R. S. Blumberg. 2008. Dependence of antibody-mediated presentation of antigen on FcRn. *Proc. Natl. Acad. Sci. USA* 105: 9337–9342.
73. Regnault, A., D. Lankar, V. Lacabanne, A. Rodriguez, C. Thery, M. Rescigno, T. Saito, S. Verbeek, C. Bonnerot, P. Ricciardi-Castagnoli, and S. Amigorena. 1999. Fcγ receptor-mediated induction of dendritic cell maturation and major histocompatibility complex class I-restricted antigen presentation after immune complex internalization. *J. Exp. Med.* 189: 371–380.
74. Rafiq, K., A. Bergtold, and R. Clynes. 2002. Immune complex-mediated antigen presentation induces tumor immunity. *J. Clin. Invest.* 110: 71–79.
75. Nimmerjahn, F., and J. V. Ravetch. 2005. Divergent immunoglobulin G subclass activity through selective Fc receptor binding. *Science* 310: 1510–1512.
76. Steinman, R. M. 2006. Linking innate to adaptive immunity through dendritic cells. *Novartis Found. Symp.* 279: 101–109.
77. Bryant, P., and H. Ploegh. 2004. Class II MHC peptide loading by the professionals. *Curr. Opin. Immunol.* 16: 96–102.
78. Pinet, V., M. Vergelli, R. Martin, O. Bakke, and E. O. Long. 1995. Antigen presentation mediated by recycling of surface HLA-DR molecules. *Nature* 375: 603–606.
79. Pinet, V. M., and E. O. Long. 1998. Peptide loading onto recycling HLA-DR molecules occurs in early endosomes. *Eur. J. Immunol.* 28: 799–804.
80. Sinnathamby, G., and L. C. Eisenlohr. 2003. Presentation by recycling MHC class II molecules of an influenza hemagglutinin-derived epitope that is revealed in the early endosome by acidification. *J. Immunol.* 170: 3504–3513.
81. Lindner, R., and E. R. Unanue. 1996. Distinct antigen MHC class II complexes generated by separate processing pathways. *EMBO J.* 15: 6910–6920.
82. Pu, Z., S. B. Lovitch, E. K. Bikoff, and E. R. Unanue. 2004. T cells distinguish MHC-peptide complexes formed in separate vesicles and edited by H2-DM. *Immunity* 20: 467–476.
83. Akilesh, S., G. J. Christianson, D. C. Roopenian, and A. S. Shaw. 2007. Neonatal FcR expression in bone marrow-derived cells functions to protect serum IgG from catabolism. *J. Immunol.* 179: 4580–4588.
84. Steinman, R. M., D. Hawiger, and M. C. Nussenzweig. 2003. Tolerogenic dendritic cells. *Annu. Rev. Immunol.* 21: 685–711.